NRC·CNRC

NRC Publications Archive
Archives des publications du CNRC

Real-time diagnosis of micro powder injection molding using integrated ultrasonic sensors

Cheng, C.-C.; Ono, Y.; Whiteside, B. D.; Brown, E. C.; Jen, C.-K.; Coates, P. D.

This publication could be one of several versions: author's original, accepted manuscript or the publisher's version. / La version de cette publication peut être l'une des suivantes : la version prépublication de l'auteur, la version acceptée du manuscrit ou la version de l'éditeur.

Publisher's version / Version de l'éditeur:

International Polymer Processing, 22, 2, pp. 140-145, 2007-01-01

NRC Publications Record / Notice d'Archives des publications de CNRC:
https://nrc-publications.canada.ca/eng/view/object/?id=1ea20e25-8b8a-4c4f-ab9c-21aed6a7b5d2
https://publications-cnrc.canada.ca/fra/voir/objet/?id=1ea20e25-8b8a-4c4f-ab9c-21aed6a7b5d2

Access and use of this website and the material on it are subject to the Terms and Conditions set forth at https://nrc-publications.canada.ca/eng/copyright
READ THESE TERMS AND CONDITIONS CAREFULLY BEFORE USING THIS WEBSITE.

L'accès à ce site Web et l'utilisation de son contenu sont assujettis aux conditions présentées dans le site https://publications-cnrc.canada.ca/fra/droits
LISEZ CES CONDITIONS ATTENTIVEMENT AVANT D'UTILISER CE SITE WEB.

Questions? Contact the NRC Publications Archive team at PublicationsArchive-ArchivesPublications@nrc-cnrc.gc.ca. If you wish to email the authors directly, please see the first page of the publication for their contact information.

Vous avez des questions? Nous pouvons vous aider. Pour communiquer directement avec un auteur, consultez la première page de la revue dans laquelle son article a été publié afin de trouver ses coordonnées. Si vous n'arrivez pas à les repérer, communiquez avec nous à PublicationsArchive-ArchivesPublications@nrc-cnrc.gc.ca.

National Research Council Canada | Conseil national de recherches Canada

Canada

Real-time Diagnosis of Micro Powder Injection Molding using Integrated Ultrasonic Sensors

C.-C. Cheng[1,*], Y. Ono[1], B.D. Whiteside[3], E.C. Brown[3], C.-K. Jen[2], and P.D. Coates[3]

IMI2006-115223-g
CNRC 48965

[1] Dept. of Electrical and Computer Engineering, McGill University, Montreal, Quebec, Canada, H3A 2A4

[2] Industrial Materials Institute, National Research Council Canada, Boucherville, Quebec, Canada, J4B 6Y4

[3] IRC in Polymer Science & Technology, University of Bradford, Bradford, UK, BD7 1DP

[*] Permanent address: Dept. of Electrical Engineering, Hsiuping Institute of Technology, Da-Li, Taichung, Taiwan

Correspondence:

Cheng-Kuei Jen

Industrial Materials Institute, National Research Council of Canada

75 de Mortagne Blvd. Boucherville, Quebec J4B 6Y4, Canada

Tel: 450-641-5086, Fax: 450-641-5106

Tel: 450-641-5085; Fax: 450-641-5106 Email: cheng-kuei.jen@cnrc-nrc.gc.ca

Abstract

Real-time diagnostics of ceramic powder injection molding using a commercial micromolding machine was performed using ultrasound. Miniature ultrasonic sensors were integrated onto the mold insert. Melt front, solidification, temperature variation and part detachment of the feedstock inside the mold cavity were observed. It has been demonstrated that ultrasonic velocity in feedstock inside the mold cavity, the ultrasonic contact duration during which the part and mold are in contact and packing/holding pressure can be used to assist with optimization of injection and cooling parameters to minimize energy consumption and maximize process efficiency.

Key words:

Miniature ultrasonic sensor, micromolding, part dimension variation, ultrasonic velocity, ultrasonic contact duration

1 Introduction

Powder injection molding (PIM) is a manufacturing process allowing mass production of complex net-shape metal or ceramic parts using feedstocks consisting of fine powders dispersed in a sacrificial (usually wax/polymer) binder. PIM components are formed using conventional injection moulding techniques to form a 'green' part which is then subjected to debinding and sintering processes to remove the binder material and achieve the required density. The process has all the benefits of conventional polymer injection molding but allows fabrication of products with superior physical properties such as high hardness, strength, and resistance to wear [1, 2, 3]. Recently micromolding technology has realized the mass production of micro-scale PIM components at a low cost [4]. However, the dimensional stability of PIM parts during the manufacturing processes needs to be

tightly controlled to ensure high quality micro components [5, 6]. The micromolding stage of the process is crucial and parameters such as melt and mold temperatures, injection and packing/holding pressures, melt volume and cooling time, need to be carefully controlled in order to produce parts which meet the required specification. Real time measurement of these parameters allows the process performance to be evaluated and can highlight defective moldings. However, integration of sensors into small and highly detailed mold units can be problematic. An ultrasonic monitoring method was chosen for this study because of its ability to measure material properties non-destructively and non-intrusively within the mold during the processing cycle [7, 8].

In this paper, miniature ultrasonic sensors have been integrated onto the mold insert of a micromolding machine for real-time process diagnosis of micro-PIM of ceramic powder. The objective of this investigation is to find ultrasonic parameters which assist with optimization of the micro-PIM process in order to improve productivity, efficiency and part quality.

2 Experiments and results

High temperature piezoelectric film ultrasonic sensors [9] were integrated onto a mold insert for operation in a commercial micromolding machine (Battenfeld Microsystem 50). These sensors can operate at temperatures up to 200°C, which is sufficiently high to encompass the full range of mould temperatures typically encountered in PIM. Fig. 1A shows the photograph of the cavity side of the mold with a mold insert, for manufacture of a circular test plaque. The cavity had a diameter of 25mm and a depth 1.5mm. This design of mold cavity is a testing one. For practical application, molder could mold micro-sized features on the mold and part surface. Fig. 1B shows a photograph of five ultrasonic transducers (UTs) fabricated directly onto the mold insert, however, only the data collected from UT1 will be presented in this paper. The insert was installed into the mobile mold of the micromolding

machine. The integrated ultrasonic sensors were 4mm in diameter and 100μm thick. Their center ultrasonic frequencies were 9-10MHz and 6dB bandwidth were 2-3MHz.

A schematic drawing of a cross-section of the mold insert showing the ultrasonic transducers and the fixed mold is given in Fig. 2. It illustrates the paths of ultrasound propagating in the mold insert and feedstock. The round trip ultrasonic longitudinal-wave echo reflected at the mold insert/ feedstock interface is indicated by L^1, and that from the surface of the fixed mold half through the feedstock is L_2.

An ultrasonic data acquisition system was composed of pulser-receivers, a 12-bit dual-channel digitizing board with a sampling rate of 50MHz for each channel, and a personal computer with data acquisition and analysis programs written using LabVIEW. The signals were acquired in a pulse-echo mode every 2ms during the entire molding cycle of 16s. In addition, the machine was equipped with piezoelectric-based load transducers for injection pressure measurements and a magnetostrictive displacement transducer for displacement and velocity measurements of the injection piston [4].

The feedstock employed was a ceramic powder (INMATEC, Rheibach) comprising aluminum oxide plus processing additives and binders. The common binders in PIM are wax / polymer mixtures. The melt feedstock (solid particles dispersed in polymer melt) was injected into the mold cavity by the injection piston in the high speed primary injection stage, after which the piston continued to inject at a much lower velocity in the packing stage, to compensate for product shrinkage during cooling and solidification. After that, the molded part was cooled down to the desired mold temperature, and then mold opened and part was ejected. A typical molding condition employed in the experiments was as follows: melt and mold temperature was 165°C and 40°C, respectively; injection and packing speed was 200mm/s and 5mm/s, respectively; packing and cooling time was 0.2s and 7.8s, respectively; and dosing amount (volume of material injected) was 820mm^3. After ejecting the part from the mold, the as-molded parts passed through the debinding and sintering processes to remove the binder and obtain the final shape. The temperature during debinding was increased from 25°C to 300°C, and during

sintering the temperature range was from 25°C to 1600°C. A photograph of an as-molded and sintered (final) part is given in Fig. 3. The black dotted circles indicate the positions of three ultrasonic transducers (UT1-3) on the mold insert, as previously shown in Fig. 1B and 2. Typical values of thickness and diameter of the as-molded and sintered part were 1.47mm and 24.8mm, and 1.26mm and 21.2mm, respectively. The average shrinkage ratio was 15%.

Fig. 4 presents the trace of ultrasonic waveforms acquired with UT1 at the mold insert (signal path shown in Fig. 2) with respect to the process time during one cycle of molding. Ultrasonic signals were acquired every 2ms during the entire cycle, but for clarity a process time interval of 70ms has been selected and shown in Fig. 4 for a cycle time of 0s to 10s. The L^1 and S echoes, propagating in the mold insert and reflected at the mold cavity surface of the mold insert, were observed to be present throughout the cycle. The signal "S" appearing at 5.9μs was ultrasonic shear-wave. The L_2 echo appeared when the feedstock arrived at the UT1 location, and remained for the duration of contact between the feedstock and the mold-cavity interface. For the data shown in Fig. 4, the time delay of the L_2 echo varied from 6.41μs at a process time of 0.77s, to 5.62μs at a process time of 9.1s. This change in delay time is directly related to changes in ultrasonic velocity and indicates the solidification and cooling of the injected feedstock material inside the mold cavity. The ultrasonic velocity increases as the feedstock solidifies. The observed phenomenon was similar with those in the conventional injection molding process and the fabrication process of microfluidic type devices described in our publications [10, 11]. The ultrasonic velocity, V_m, inside the mold cavity can be determined by $V_m = 2h_m/\Delta t_m$, where h_m is the depth of the cavity at the transducer location and Δt_m is the time delay difference between the L^1 and L_2 echoes as observed in Fig. 4.

Fig. 5A and 5B present both the amplitude of the L^1 echo (measured using UT1 at the mold insert), and the injection pressure measured by a pressure sensor installed at the end of the injection piston for typical molding cases. In Fig. 5A, at a process time of 0.34s an increase in injection

pressure was observed, indicating entry of the feedstock into the mold cavity. At a process time of 0.77s, the end of injection stage, the magnitude of injection pressure reached the first of two peaks, and the feedstock arrived at the location of UT1, as evidenced by a sharp decrease in the amplitude of the L^1 echo. This amplitude decreased because a proportion of the ultrasonic energy which had previously been reflected back to the transducer when the cavity was empty, was transmitted into the feedstock through the mold. After a process time of 0.77s the amplitude of the L^1 echo gradually decreased further, due to densification during packing. At a process time of 1.7s, which correlates to the end of the packing stage, the injection pressure reached a second peak value and the L^1 echo amplitude reached a minimum value which was maintained throughout the remainder of the cycle until part detachment. At a process time of 9.1s, the amplitude of the L^1 echo recovered to the initial value due to total reflection at the mold insert/air interface, indicating that the mold had opened and the molded part was detached from the surface of the mold cavity. In some cases, as shown in Fig. 5B, it is possible for part shrinkage to cause detachment to occur before the mold opens, evidenced at a process time of 5s in Fig. 5B, thereby limiting the efficacy of the mold in cooling the part and implying the possibility of reducing cycle time. The amplitude of the L^1 echo can be used to aid this by indicating part detachment in-situ before mold opening.

In the first set of experiments described (sections 3.1~3.4), the fabrication of micro-PIM parts was carried out with a constant material dose set to 820mm^3 and at an injection speed of 200mm/s. During the packing stage, different packing speeds of 3, 5, 7, and 9mm/s were selected for an injection piston displacement of 1mm in order to investigate the effect of changes in packing parameters. The range of packing speeds was selected to avoid incomplete filling or flashing. In the second set of experiments described (section 3.5), the fabrication process was carried out with the same material dose set of 820mm^3 and at different injection speeds of 150, 200, 250, and 300mm/s in order to investigate the effect of changes in injecting parameters. During the packing stage, a packing speed of 5mm/s was selected.

3 Discussions

3.1 Evaluation of part thickness and weight

To evaluate the quality of these parts, the thickness of as-molded and sintered parts was measured using a micrometer with stated accuracy of ±1μm, and the weight by a balance with stated accuracy of ±2mg. The results are shown in Fig. 6. The open (e.g. ○) and filled (e.g. ●) symbols represent as-molded and sintered parts, respectively. The straight lines for these two sets of symbols were obtained by a least square fitting method. In the thickness range of 1.452mm to 1.484mm and 1.235mm to 1.292mm for the as-molded and sintered parts, respectively, the weight increases linearly from 1.951g to 2.024g for the as-molded parts, with density of 2.78±0.009 (±0.33%) g/cm^3. The densities of as-molded parts were measured by Archimedes method. The values were within our measurement error and didn't have clear correlation with packing speed. In this figure, we can also compare the shrinkage of thickness for each part. Due to our un-optimal debinding-and-sintering process at present time, the diversion of thickness for sintered parts is larger than that of as-molded parts. In Fig. 6 the maximum thickness differences of all as-molded and sintered parts were 32μm and 57μm, respectively. This difference may exceed the desired specification of the micro PIM parts, e.g. the required accuracy of some special clock components was ±5μm. Furthermore the dimension inconsistency may be a serious problem when parts dimensions are small, e.g. the required diameter of a gearwheel was 257μm [5,6]. Part thickness and weight showed no correlation with packing speed, as shown in Fig. 6. Differences in part thickness and weight evident in Fig. 6 for as-molded parts are likely to have been caused by inconsistent dosing during each fabrication cycle even with the same machine setting of 820mm^3.

3.2 Correlation of ultrasonic velocity with part thickness

To verify our assumption that the inconsistencies in part thickness and weight were due to poor dosing repeatability, simple molding experiments using two different machine dosing settings of 820mm^3 and 850mm^3 were conducted. In these experiments no packing speed was applied. The ultrasonic velocity in the part was obtained at a processing time of 1s, where process time was defined to start when the injection piston movement began. The measurement at the processing time 1s was chosen because the part detached from mold surface after 1.5s for most cases and the temperature, which will affect the ultrasonic velocity in the part, was expected to have little variation with this timing. The relationships between measured ultrasonic velocity and part thickness and weight were shown in Fig. 7 where it was apparent that part thickness and weight increased with increasing dosing volume. Small differences in part thickness and weight might have been caused by minor differences in dosing under the same machine setting. Ultrasonic velocity is sensitive to pressure. The cavity pressure would be higher when there was more material inside the cavity during molding process. Therefore, the data in Fig. 7 also provided an indication that ultrasonic velocity may be able to relate with the part thickness and weight. However, in these simple experiments no packing speed was applied.

Typically during the micro-PIM process, a packing speed is applied to aid packing. Ultrasonic velocity had been determined for each of the parts shown in Fig. 6 at a processing time of 1s. The choice of 1s was because many parts detached from mold surface after 1.5s, and the fixed timing would cause less temperature variation. The relationships between the ultrasonic velocity and the measured part thickness and weight were shown in Fig. 8. There is a linear relationship existed between them. The standard deviations in thickness and weight of as-molded parts were ±2.3μm and ±4.6mg, respectively. This strongly suggests that ultrasonic velocity may be a parameter related to the

thickness and weight of the fabricated micro PIM parts. Part thickness changed over time due to shrinkage. The thicknesses of all parts were less than the cavity depth of 1.5 mm.

3.3 Correlation of cooling efficiency with part thickness

Ultrasonic contact duration in Fig. 5 indicates the period during which the part and mold are in contact and helps in evaluation of the cooling efficiency. A consistent contact duration implies a uniform cooling profile, and may help repeatability of final part properties as illustrated below. The contact duration is defined as occurring between melt arrival and mold opening or part detachment. The contact duration measured by the L^1 echo at the UT1 position was compared with the part thickness measured at the UT1 location and the results are shown in Fig. 9. The standard deviations in thickness of as-molded and sintered parts were ±4.6 μm and ±12.1μm, respectively. It is noted that, due to our un-optimal debinding-and-sintering process at present time, the standard deviation in thickness of sintered parts is larger than that of as-molded ones. In Fig.9, all the parts were identical to those shown in Fig.6. It implies that if one can maintain a constant ultrasonic contact duration, the weight and thickness variations of the PIM parts may be reduced. For instance, the two parts of a and b, shown in Fig.9 (and Fig.6), their contact durations were 8.4s. Their thicknesses are 1.481±0.003mm and 1.287±0.005mm for the as-molded and sintered parts, respectively. Fig. 9 suggests that ultrasonic contact duration may be another parameter to assist the consistency of part thickness of as-molded and sintered parts during the PIM process. However the deviation in part thickness versus ultrasonic velocity in the part shown in Fig.8 (±2.3μm) is better than that versus ultrasonic contact duration shown in Fig.9 (±4.6 μm).

3.4 Effects of pressure

It is our intention to adjust packing pressure at the end of packing stage by change the packing speed and to evaluate the effects. For all the parts made in Fig.6 under the same dosing amount setting of 820mm^3 and the same injection speed of 200mm/s but with different packing speeds (3, 5, 7, 9mm/s) for a further injection piston movement of 1mm. The experimental results show us there is no correlation between the packing speed and the packing pressure.

The relationship between the measured packing pressures versus the part thickness for all as-molded parts in Fig.6 was presented in Fig.10. The standard deviation in thickness of as-molded parts was ±4.8 μm. The data suggests that a higher injection pressure, which is a function of injection speed and dosing volume, leads to an increase in part thickness. However the deviation in part thickness versus ultrasonic velocity in the part shown in Fig.8 (±2.3μm) is better than that versus packing pressure shown in Fig.10 (±4.8 μm).

During these experiments there was no cavity pressure sensor installed. Since commercially available sensors need to be in direct contact with the part, holes must be machined in the mold inserts in order to accommodate them, and they may not withstand the conditions of friction and high pressures in the cavity. The integrated ultrasonic sensors presented here are non-invasive and provide an advantageous alternative to conventional intrusive piezoelectric-based or capacitance-based pressure sensors.

3.5 Evaluation of injection speed

The effect of changing injection pressure by adjustment of the injection speed has been evaluated. Four injection speeds were selected, namely 150, 200, 250, 300m/s. Dosing volume was set to 820mm^3 and a constant packing speed of 5mm/s (for a further injection piston displacement of 1mm) was set. Fig.

12 presents the relationship between the injection speed and the injection pressure. Injection pressure increased with injection speed but there was considerable scatter. The thickness of as-molded parts was measured for comparison with injection speed. The experimental results show us there is no clear correlation between injection speed and part thickness of as-molded parts, which indicates that injection and packing speeds cannot be used to optimize part dimension.

4 Conclusions

Real-time, non-intrusive and non-destructive process monitoring of micro PIM has been performed using integrated high temperature ultrasonic sensors. The ultrasonic sensors were fabricated directly onto the mold insert of the micromolding machine. Ultrasonic monitoring of micro PIM part of around 24.8mm-diameter and 1.47mm-thick was demonstrated with an aluminum oxide feedstock. Melt front, solidification, part temperature, and part detachment of the feedstock inside the mold cavity were observed.

It was found that the machine operated under the same injection speed and setting of dosing amount produced the parts with significant variation in part thickness measured by a micrometer and weight measured by a balance. Our experiments data indicated that the difference in part thickness and weight might be caused by the different actual dosing amounts.

This investigation indicated that there exists a correlation between the part thickness versus (1) ultrasonic velocity measured at the processing time of 1s, and (2) ultrasonic contact duration in which the part and mold are in contact, and (3) packing pressure shown in Fig.5. If these parameters can be controlled and improved, part dimension tolerance might be met. However, the correlation between the ultrasonic velocity in the feedstock versus part thickness is the best among the three. Therefore it is demonstrated that the presented integrated ultrasonic sensors and technique might be an excellent approach to optimize the micro PIM process, and reduce the part dimension variation.

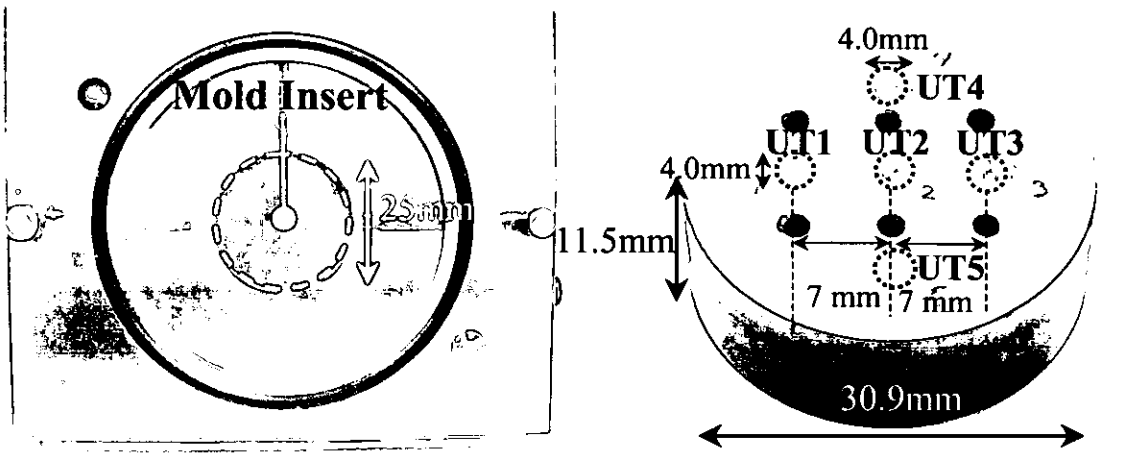

Fig. 1. Photographs of A) a mold with the mold insert (indicated by white dotted circle area) at cavity side and B) a mold insert with five UTs at UT side.

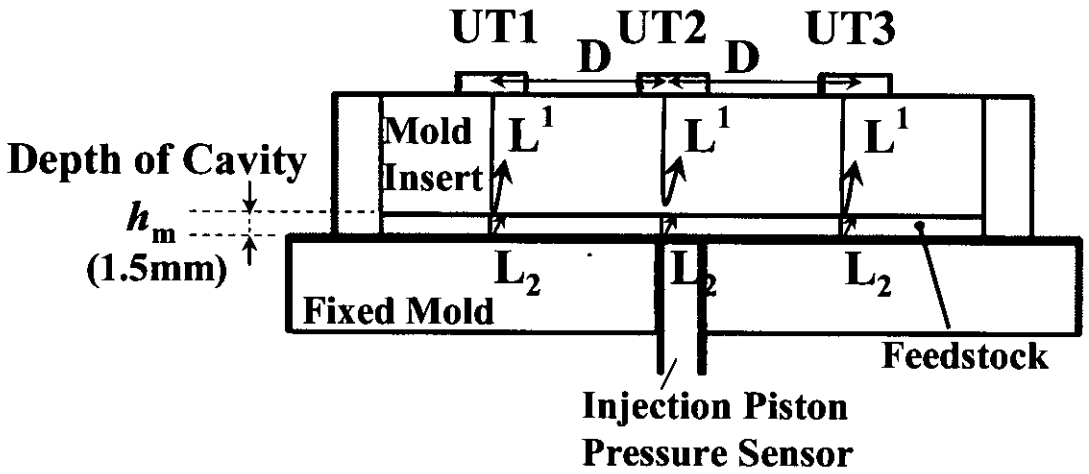

Fig. 2. Cross-sectional view of the mold insert with the UTs and the paths of ultrasonic signals propagating in the mold insert and feedstock. The cavity had a diameter of 25mm and a depth of 1.5mm.

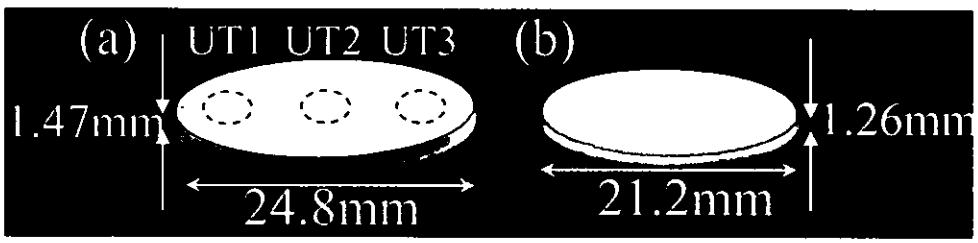

Fig. 3. Photograph of (a) an as-molded part and (b) a sintered part. The black dotted circles indicate the location of the UT1-3.

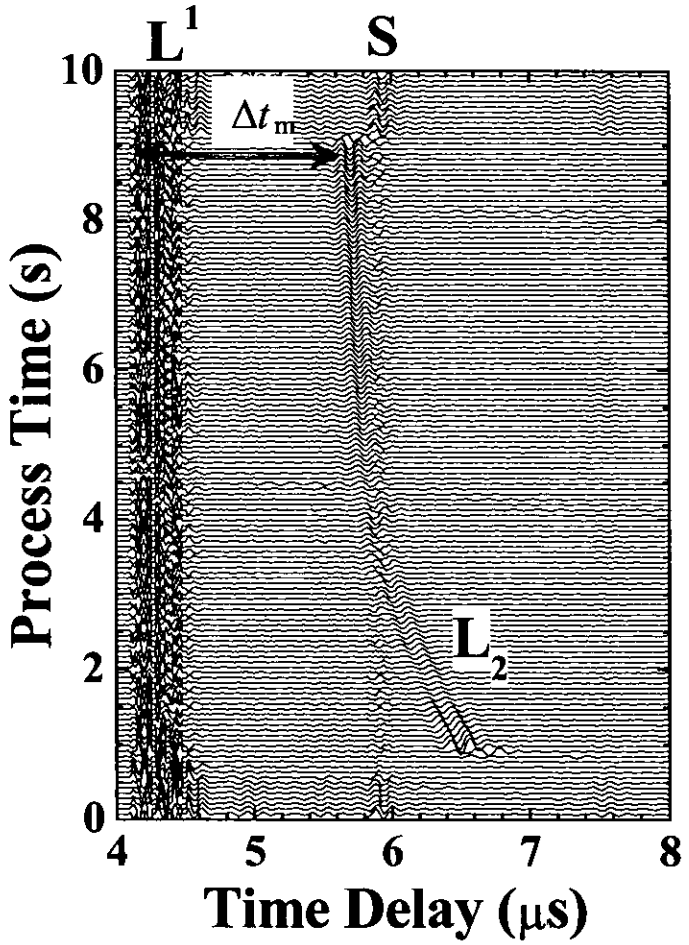

Fig. 4. Typical signal measured with the UT1 shown in Fig.1(b) during one cycle of molding.

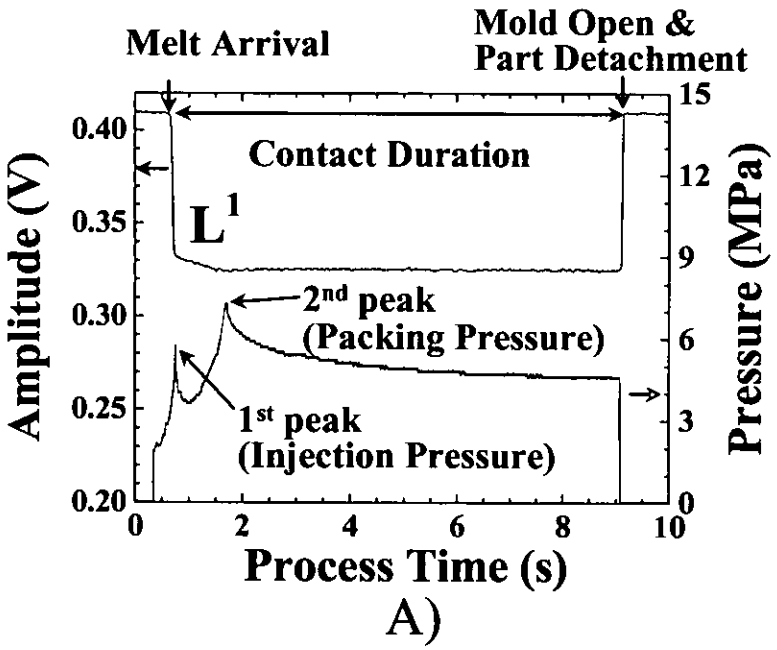

Fig. 5A. Amplitude variations of the L^1 echo reflected at mold insert/feedstock interface measured using the UT1 and pressure measured by a pressure sensor. These signals were acquired for the part keeping contact with mold surface until mold open.

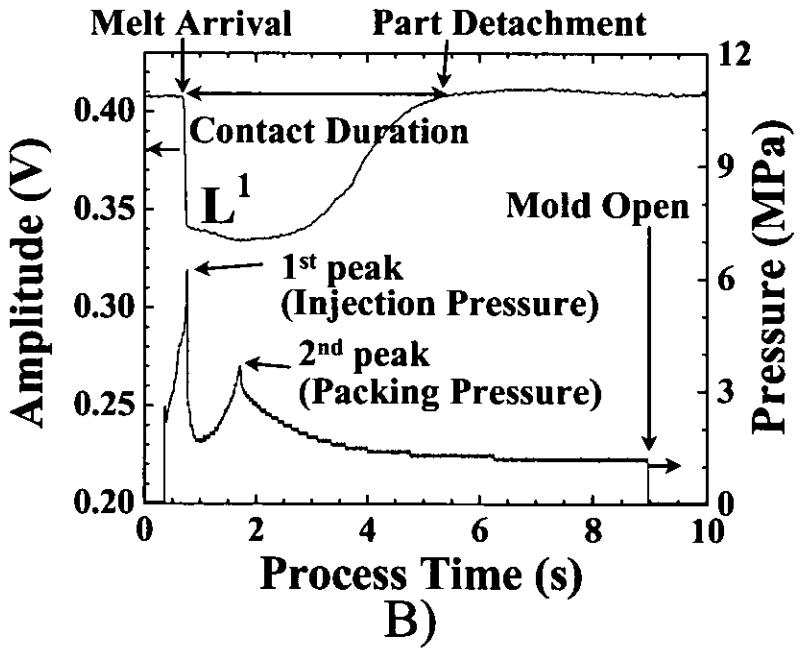

B)

Fig. 5B. Amplitude variations of the L^1 echo reflected at mold insert/feedstock interface measured using the UT1 and pressure measured by a pressure sensor. These signals were acquired for the part detached from the mold surface before mold open.

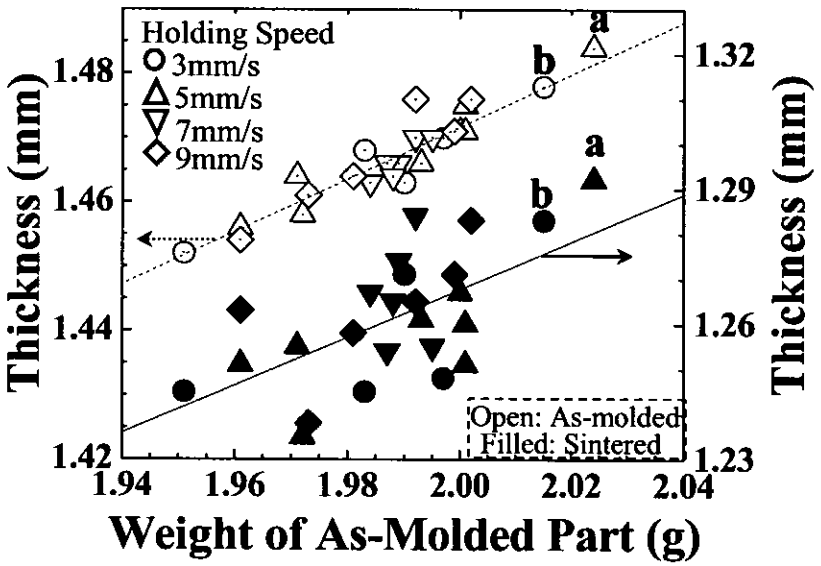

Fig. 6. Thickness of as-molded (open symbols) and sintered (filled symbols) parts, measured by a micrometer at UT1 location in Fig. 1(b), with respect to weight of as-molded part measured by a balance. Dosing amount setting was 820mm^3.

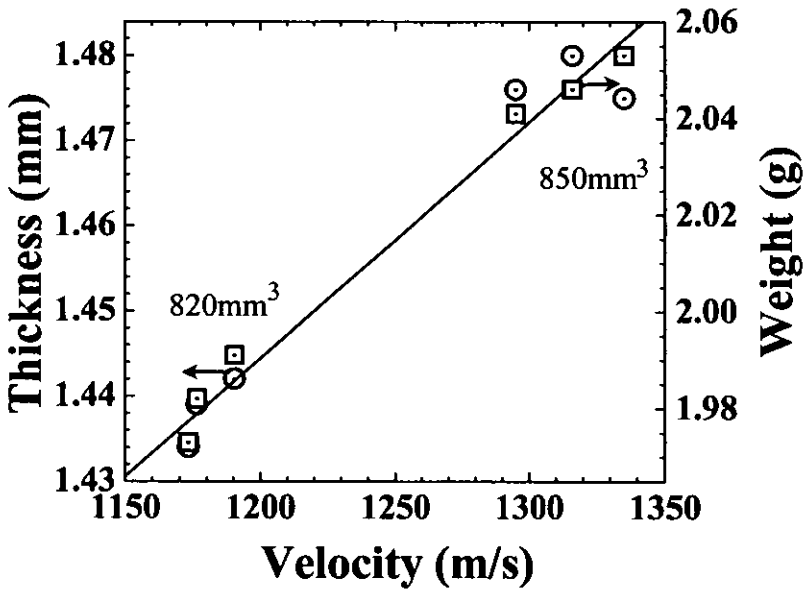

Fig. 7. Thickness and weight of as-molded parts at different dosing amount settings with respect to ultrasonic velocity in feedstock at the processing time of 1s in Fig. 5.

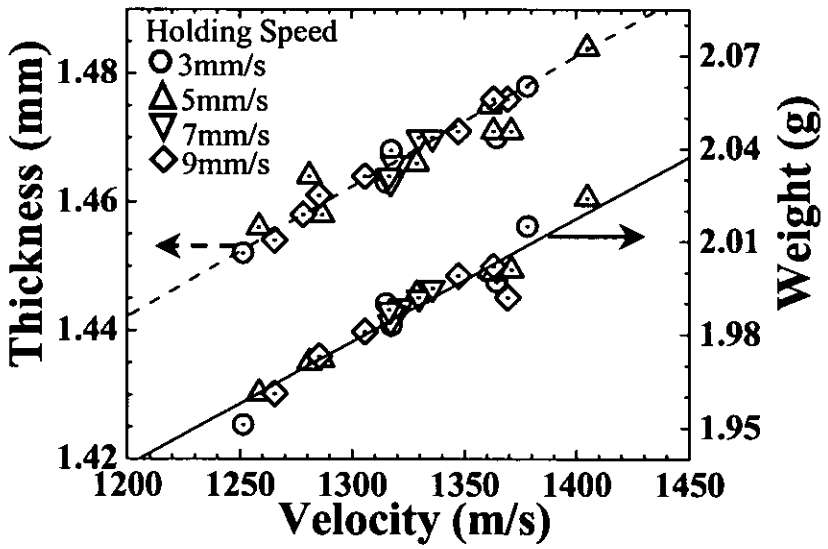

Fig. 8. Thickness and weight of as-molded parts with respect to ultrasonic velocity in feedstock at the processing time of 1s in Fig. 5. The parts are the same as those in Fig.6.

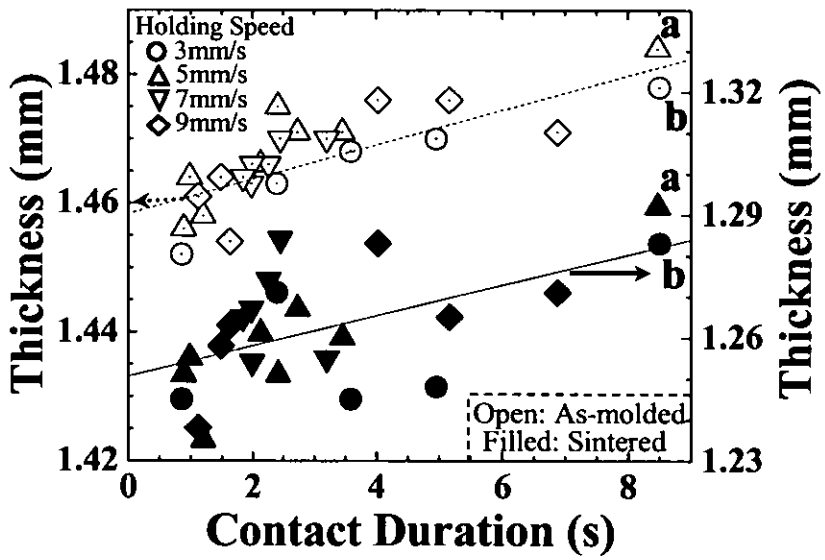

Fig. 9. Thickness of as-molded (open symbols) and sintered (filled symbols) parts with respect to ultrasonic contact duration of L^1 echo measured by the UT1 in Fig. 2. The parts are the same as those in Fig.6.

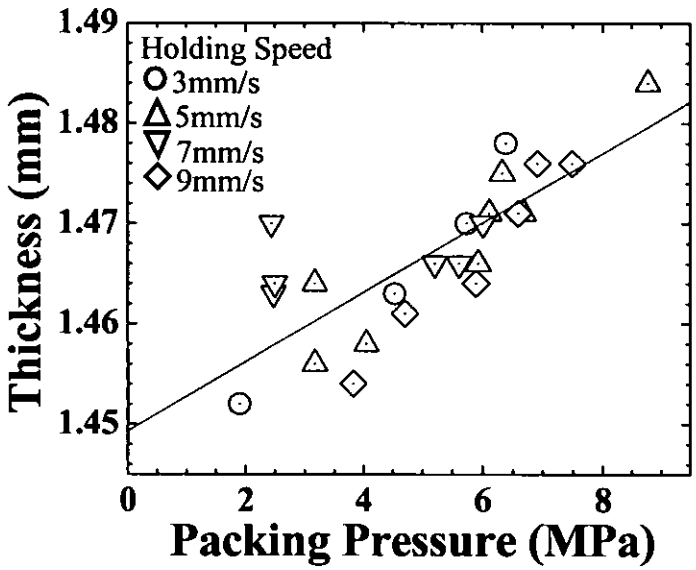

Fig. 10. Thickness of as-molded parts versus the packing pressure in Fig. 5.

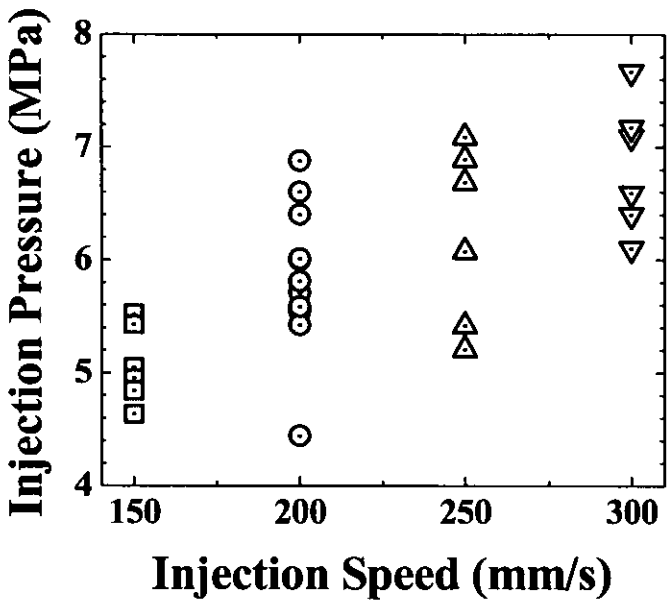

Fig. 11. Injection pressure in Fig. 5 versus different injection speeds.

References

[1] German, R.M., in: Powder Injection Molding: Design and Application. Innovative material solutions Inc. Publishers, State College, PA, p. 1/8 (2003)

[2] Piotter, V., Benzler, T., Gietzelt, T., Ruprecht, R., Haubelt, J.: Adv. Engineer. Materials 10, p. 639 (2000)

[3] Gietzelt, T., Piotter, V., Jacobi, O., Riprecht, R., Hausselt, J.: Adv. Engineer. Materials 5, p. 139 (2003)

[4] Whiteside, B.R., Martyn, M.T., Coates, P.D., Allan,P.S., Hornsby, P.R., Greenway, G.: Plastics, Rubber and Composites 32, p. 231 (2003)

[5] Yoshikawa, K., Ohmori, H.: RIKEN 34, p. 13 (2001)

[6] Piotter, V., Bauer, W., Benzler, T., Emde,A.: Microsystem Technologies 7, p. 99 (2001)

[7] Hongerholt, D.D., Rose, J.L., German, R. M.: JOM 9, p. 24 (1996)

[8] Hongerholt, D.D., Rose, J.L., German, R.M.: NDT&E International 30, p. 389 (1997)

[9] Kobayashi M., Jen, C.-K.: Smart Materials and Structures 13, p. 951 (2004)

[10] Ono, Y., Cheng, C.-C., Kobayashi, M., Jen, C.-K.: Poly. Eng. and Sci. 45, p. 606 (2005)

[11] Kobayashi, M., Ono, Y., Jen, C.-K, Cheng, C.-C.: IEEE Sensors Journal 6, p. 55 (2006)

Acknowledgments

The author would like to thank M. Kobayashi for fabricating the UTs, and Y. Thomos, S. Vicky and S. Mercier for technical assistance in PIM experiments. Financial supports of Joint Science and Technology Fund of National Research Council of Canada and British Council, and the Natural Sciences and Engineering Research Council of Canada are acknowledged.